



**HAL**  
open science

# Robust intrathymic development of regulatory T cells in young NOD mice is rapidly restrained by recirculating cells

Julie Darrigues, Jeremy C Santamaria, Ariel Galindo-albarrán, Ellen A Robey, Olivier P Joffre, Joost P M van Meerwijk, Paola Romagnoli

► **To cite this version:**

Julie Darrigues, Jeremy C Santamaria, Ariel Galindo-albarrán, Ellen A Robey, Olivier P Joffre, et al.. Robust intrathymic development of regulatory T cells in young NOD mice is rapidly restrained by recirculating cells. *European Journal of Immunology*, 2020, 51 (3), pp.580 - 593. 10.1002/eji.202048743 . inserm-04670667

**HAL Id: inserm-04670667**

**<https://inserm.hal.science/inserm-04670667v1>**

Submitted on 12 Aug 2024

**HAL** is a multi-disciplinary open access archive for the deposit and dissemination of scientific research documents, whether they are published or not. The documents may come from teaching and research institutions in France or abroad, or from public or private research centers.

L'archive ouverte pluridisciplinaire **HAL**, est destinée au dépôt et à la diffusion de documents scientifiques de niveau recherche, publiés ou non, émanant des établissements d'enseignement et de recherche français ou étrangers, des laboratoires publics ou privés.










Distributed under a Creative Commons Attribution 4.0 International License



## Research Article

# Robust intrathymic development of regulatory T cells in young NOD mice is rapidly restrained by recirculating cells

Julie Darrigues\*<sup>1</sup> , Jeremy C. Santamaria\*<sup>1</sup> ,  
Ariel Galindo-Albarrán<sup>1,2</sup> , Ellen A. Robey<sup>3</sup> , Olivier P. Joffre<sup>1</sup> ,  
Joost P.M. van Meerwijk<sup>1</sup>  and Paola Romagnoli<sup>1</sup> 

<sup>1</sup> Centre de Physiopathologie Toulouse Purpan (CPTP), Inserm U1043, CNRS UMR 5282, Université de Toulouse III (UPS), Toulouse, France

<sup>2</sup> Station d'Ecologie Théorique et Expérimentale, CNRS, Moulis, France, Université Paul Sabatier, Moulis, France

<sup>3</sup> Division of Immunology and Pathogenesis, Department of Molecular and Cell Biology, University of California, Berkeley, CA

Regulatory T lymphocytes (Treg) play a vital role in the protection of the organism against autoimmune pathology. It is therefore paradoxical that comparatively large numbers of Treg were found in the thymus of type I diabetes-prone NOD mice. The Treg population in the thymus is composed of newly developing cells and cells that had recirculated from the periphery back to the thymus. We here demonstrate that exceptionally large numbers of Treg develop in the thymus of young, but not adult, NOD mice. Once emigrated from the thymus, an unusually large proportion of these Treg is activated in the periphery, which causes a particularly abundant accumulation of recirculating Treg in the thymus. These cells then rapidly inhibit *de novo* development of Treg. The proportions of developing Treg thus reach levels similar to or lower than those found in most other, type 1 diabetes-resistant, inbred mouse strains. Thus, in adult NOD mice the particularly large Treg-niche is actually composed of mostly recirculating cells and only few newly developing Treg.

**Keywords:** inbred mouse strains · regulatory T cells · thymic niche · thymus · tolerance



Additional supporting information may be found online in the Supporting Information section at the end of the article.

## Introduction

Regulatory T lymphocytes (Treg) expressing the transcription factor Foxp3 are major actors in the control of immune-responses to self- and non-self [1,2] and of tissue integrity [3]. Their absence in humans and mice carrying mutations in the *FOXP3/Foxp3*

locus leads to lethal pathology early in life [4,5], best illustrating their central role in immune-tolerance. Whereas Treg can also differentiate from conventional T cells (Tconv) in the periphery, the work of several laboratories highlights the importance of thymus-derived Treg in protecting the organism from fatal immune-pathology [6]. In the thymus, at least three factors

**Correspondence:** Prof. Joost P.M. van Meerwijk  
e-mail: Joost.van-Meerwijk@inserm.fr

\*Darrigues and Santamaria contributed equally.  
[Correction added on 17 August 2020, after first online publication: URL for peer review history has been corrected.]

govern the development of Treg: high affinity interactions of TCRs expressed by developing thymocytes with peptide/MHC ligands expressed by thymic stromal cells [7]; costimulatory [8–10] and adhesion molecules [11]; and signals downstream of cytokine-receptors [12]. Combined, these factors establish a thymic niche dedicated to Treg development.

Using transgenic mice expressing GFP under the control of the *Rag2* promoter [13], others and we recently showed that two distinct Treg populations occupy the thymic Treg niche: developing (GFP<sup>+</sup>) and fully mature (GFP<sup>-</sup>) cells [14–16]. GFP<sup>-</sup> thymic Treg comprise a population of differentiated and suppressive cells recirculating from the periphery back to the thymus [15]. Mature thymic Treg can inhibit de novo Treg development by limiting the bioavailability of IL-2 [15,17], and apparently also favor Treg development by neutralizing IL-1 $\beta$  [18]. The proportion of recirculating effector/memory Treg strongly increases with age. These cells already represent almost half of the thymic Treg pool in 8-wk-old C57BL/6 mice and fill the entire thymic Treg-niche in 1-year-old mice. In parallel, thymic production of Treg, but not Tconv, drastically drops, showing an age-dependent regulation of Treg development [15].

Several studies have shown quantitative differences in the proportion and numbers of thymic Treg in common inbred laboratory mouse strains leading to the description of quantitative trait loci (QTL) determining the size of the thymic Treg niche [19–22]. One of the major quantitative differences was observed between the type I diabetes-prone non-obese diabetic (NOD) mice which, paradoxically, have a large thymic Treg niche, and C57BL/6 (B6) mice, which are resistant to autoimmune-disease and present a relatively small Treg-niche [19,22]. Results obtained with in vitro thymus organ cultures suggested that more Treg develop de novo in NOD than in B6 mice, but in vivo data are still lacking.

In light of the described heterogeneity of the population of thymic Treg [14,15] and of the inhibition that recirculating peripheral Treg exert on de novo development of Treg [15], we revisited thymic development of Treg in several inbred mouse strains, with a particular emphasis on NOD and B6 mice, using approaches allowing rigorous distinction between developing and recirculating Treg.

## Results

### The NOD thymus has a particularly large Treg-niche

In this study, as in our previously published work [15], we defined Treg as Foxp3<sup>+</sup> cells, irrespective of CD25-expression. This is based on the observation that CD25<sup>-</sup> Treg with suppressive functions have been reported in the periphery [23,24], and that we found substantial proportions of CD25<sup>-</sup> Treg among recent thymic emigrants (defined as GFP<sup>+</sup> cells in *Rag2-Gfp* transgenic mice) and among more mature (GFP<sup>-</sup>) Treg in the spleen (Supporting Information Fig. S1A).

Previous work showed that the thymic Treg niche is greater in NOD than in B6 mice [19,22]. To assess if NOD mice have a particularly large or B6 mice, a particularly small Treg niche, we analyzed Treg-development in the thymus of eight inbred mouse strains at 8 weeks of age. We found the highest proportion of Treg in NOD mice, only rivalled by that found in the CBA thymus (Fig. 1A; Supporting Information Fig. S1B). B6 mice had the smallest proportion of Treg among mature CD4SP thymocytes. These results establish that inbred mouse strains exhibit a range of thymic Treg frequencies, with NOD and B6 mice representing the high and low extremes respectively of this range.

### NOD thymocytes have a high capacity to differentiate into Treg

To assess if the relatively large Treg niche in NOD mice correlates with a stronger development of these cells, we next analyzed the proportions of Treg among mature CD4SP cells in the thymus of three-day old mice, i.e., before newly developing Treg leave the thymus and therefore before peripheral Treg recirculate back to the thymus and inhibit Treg-differentiation. The data on eight inbred mouse strains show that NOD mice have among the highest and B6 mice among the lowest levels of newly developing Treg (Fig. 1B), which corresponds to the sizes of the Treg-niche observed at 8 weeks (Fig. 1A). However, whereas in some strains the levels of newly developing Treg at 3 days of age correlated with the size of the Treg-niche at 8 weeks (B6, BALB/c, DBA/1, CBA, NOD), in the other strains it did not (SJL, FVB/N, C3H; cf. Fig. 1A and B; Supporting Information Fig. S1C). This observation suggested that in the distinct inbred mouse-strains the Treg niche in adult mice is composed of different proportions of newly developing versus recirculating Treg.

### Differences in the proportions of recirculating Tregs in the thymi of inbred mouse strains

To analyze the proportions of newly developing and recirculating Treg in the thymi of adult WT mice, we first searched for cell-surface markers that allow for their identification. These two populations can reliably be distinguished using mice carrying the *Rag2-Gfp* and *Foxp3-Thy1a* reporters [15,25]. We found that a CCR7<sup>high</sup>CD73<sup>-/low</sup> phenotype best corresponded to newly developing (i.e., GFP<sup>+</sup>) Treg and a CCR7<sup>-/low</sup>CD73<sup>high</sup> phenotype to recirculating (GFP<sup>-</sup>) Treg in both B6 and NOD mice (Fig. 1C). Using this definition, we found substantial differences in the proportions of recirculating Treg in thymi from adult mice of the studied inbred strains (Fig. 1D; Supporting Information Fig. S1D). While some strains (e.g., CBA, C3H, BALB/c) had relatively few recirculating Tregs at 8 weeks of age, others (e.g., NOD, FVB/N, SJL) had a large proportion of recirculating Tregs at this time point. Importantly, these differences in the proportions of

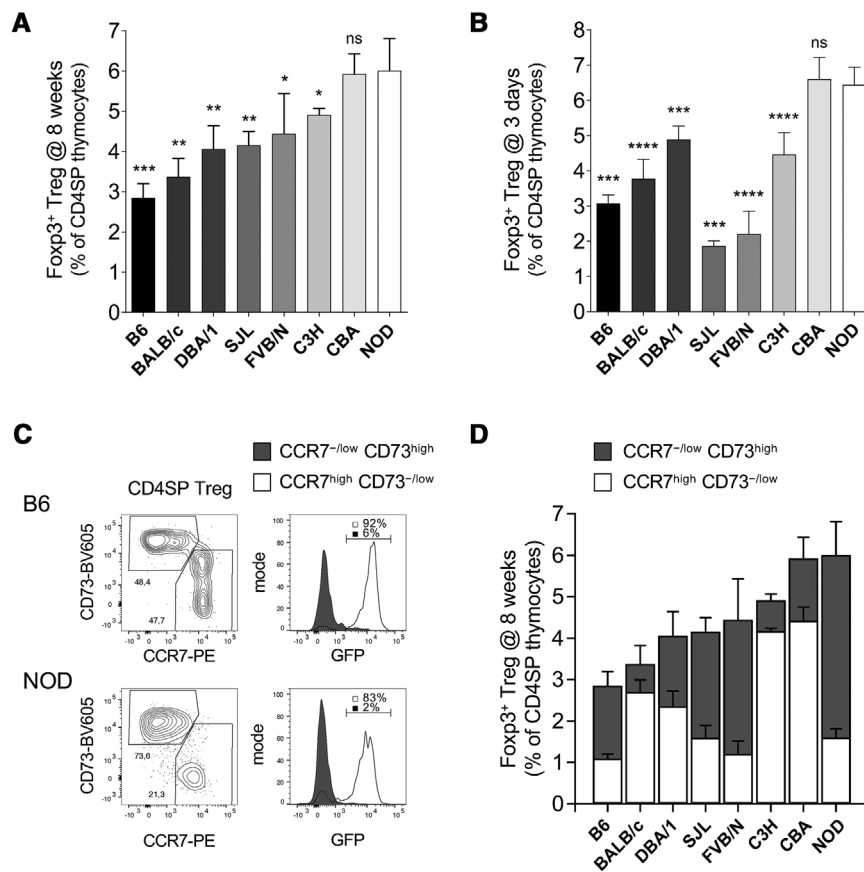


**Figure 1.** Comparatively large Treg-niche and strong Treg-development in the NOD thymus. Thymocytes from indicated inbred mouse strains were analyzed by flow-cytometry using antibodies to indicated markers. Proportions of Foxp3<sup>+</sup> cells among CD4<sup>+</sup>CD8<sup>-</sup>TCR<sup>high</sup> (CD4SP) thymocytes from (A) 8-week- or (B) 3-day-old mice. (C) Thymocytes from *Rag2-Gfp Foxp3-Thy1a* B6 mice were analyzed by flow-cytometry. Left panel: CCR7 versus CD73 expression by CD4SP Foxp3<sup>+</sup> Treg. Right panel: GFP-levels on cells gated as indicated in the left panel. Data from a representative experiment out of more than four performed is shown. (D) Thymocytes from 8-week-old WT mice of the indicated inbred strains ( $n \geq 5$ /strain) were analyzed by flow-cytometry and proportions of recirculating CCR7<sup>low</sup>CD73<sup>high</sup> Treg and of newly developing CCR7<sup>high</sup>CD73<sup>low</sup> Treg were determined. Five to nine mice were analyzed for each strain at 8 weeks in two to three independent experiments. Five to 13 mice were analyzed for each strain at 3 days in two independent experiments. Mean values  $\pm$  SD. ns, not significant; \* $p < 0.05$ ; \*\* $p < 0.01$ ; \*\*\* $p < 0.001$ ; \*\*\*\* $p < 0.0001$  (Mann-Whitney test), as compared to NOD thymocytes.

recirculating Treg at 8 weeks of age did not correlate with those observed in the proportions of newly developing cells in 3-day-old mice (Fig. S1E). They therefore apparently were not caused by the differences in the initial thymic production of Treg. These data suggest that two distinct factors, the overall size of the thymic Treg niche, and the propensity for recirculation of mature Tregs to the thymus, independently contribute to distinct thymic Treg compartments in different inbred mouse strains.

### The development of Treg in NOD thymi evolves dynamically with age

The observation that newly developing Tregs were found in greater proportions in NOD than in B6 mice at 3 days, but not at 8 weeks of life (Fig. 1B and D) suggests a dynamic change in thymic Treg production in early life. To explore this phenomenon in further detail, we performed a longitudinal analysis of the proportions of Treg cells among newly developing (GFP<sup>+</sup>) mature CD4SP thymocytes from *Rag2-Gfp Foxp3-Thy1a* mutant B6 and NOD mice (Fig. 2A and B; Supporting Information Fig. S2A). Similar to our observations in 3-day old mice (Fig. 1B), we observed a substantially greater proportion of newly developing Treg in NOD than in B6 thymi at 2- and 3-weeks of age. However, later on the proportions of newly developing Treg cells rapidly declined in NOD mice and became comparable to those in B6 animals

(Fig. 2B). Analysis of absolute numbers yielded similar results (Supporting Information Fig. S2B).

### Particularly high levels of recirculating Treg accumulate in the NOD thymus

We next investigated the mechanisms involved in this drop in Treg development in NOD thymi. We previously showed that mature Treg that had recirculated to the thymus inhibit de novo Treg-differentiation [15]. We therefore assessed the levels of recirculating NOD and B6 cells in the thymic medulla, the site of Treg differentiation, of NOD and B6 mice. We first performed an analysis of the proportion of recirculating (GFP<sup>-</sup>) mature Foxp3<sup>+</sup> Treg among CD4SP thymocytes in 2- to 8-week-old NOD and B6 mice. Substantially higher levels of recirculating Treg were observed in NOD than in B6 thymi all along the studied time-course (Fig. 2C and D; Supporting Information Fig. S2C). Importantly, the ratio of recirculating to newly developing Treg was substantially higher in NOD than in B6 mice (Supporting Information Fig. S2D). This result demonstrates that the higher level of recirculating Treg in NOD than in B6 mice is not solely due to the larger Treg-production by the NOD thymus. It thus consolidates our conclusion that the differences in recirculation we observed in the eight studied inbred mouse strains apparently is not due to the initial thymic output of Treg (Supporting Information Fig. S1E). Also, the proportions

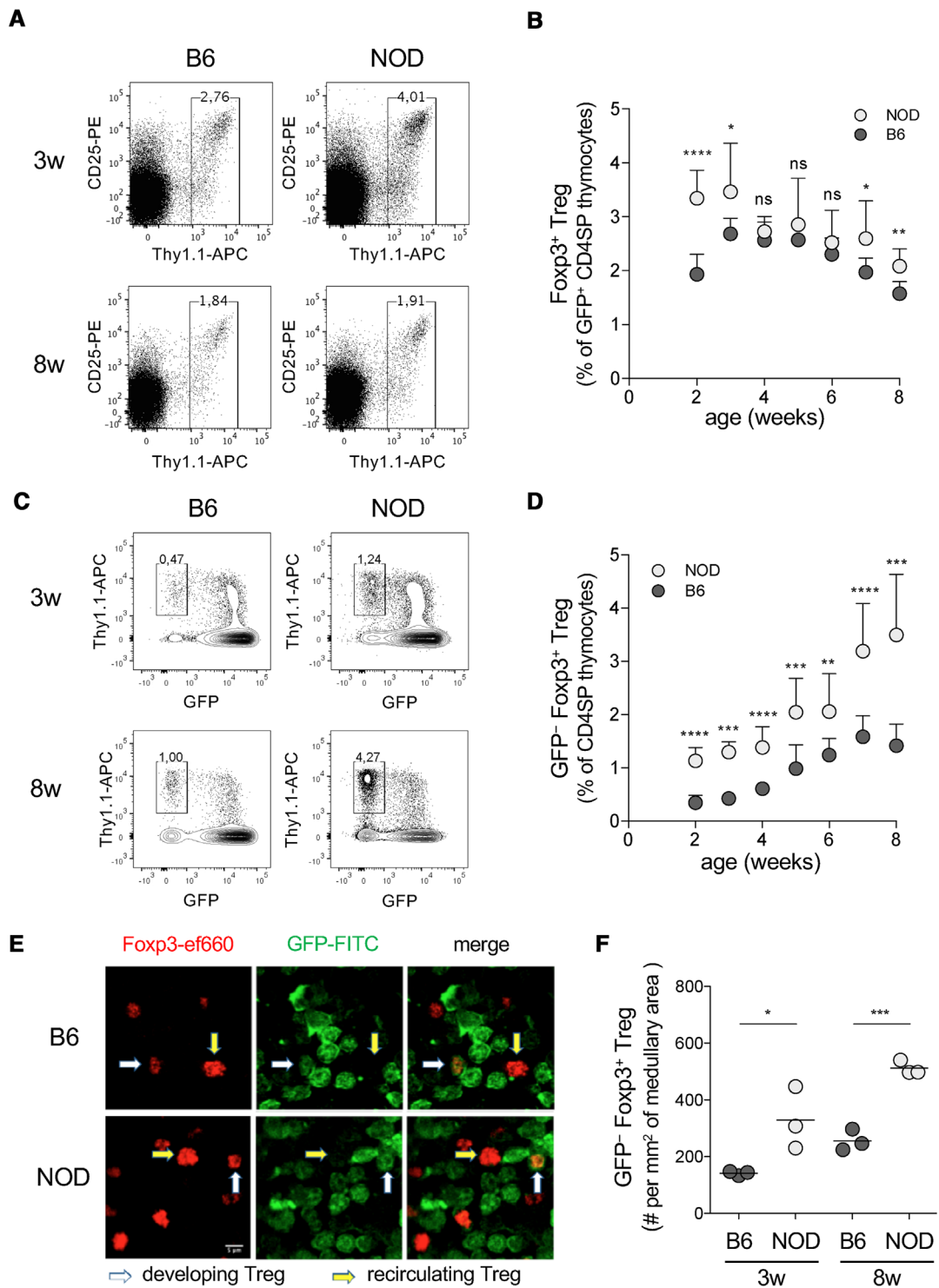


**Figure 2.** Dynamic changes in the composition of the Treg niche during the first weeks of age. Thymocytes from *Rag2-Gfp Foxp3-Thy1a* NOD and B6 mice were analyzed by flow-cytometry and confocal microscopy using antibodies to indicated markers. (A) Thymocytes were from 3- and 8-week-old NOD and B6 mice, as indicated. Shown is the expression of Thy1.1 versus CD25 on CD4<sup>+</sup>CD8<sup>-</sup>TCR<sup>high</sup>GFP<sup>+</sup> thymocytes, gated as in Supporting Information Fig. S2A. Depicted gates were used to quantify newly developing Treg. (B) Quantification of developing Treg. Each symbol represents the mean of 7–14 individual measurements  $\pm$  SD, pooled from one to four independent experiments per time-point. See Supporting Information Fig. S2B for absolute numbers. (C) Thymocytes were from 3- and 8-week-old NOD and B6 mice, as indicated. Shown is the expression of GFP vs. Thy1.1 on CD4<sup>+</sup>CD8<sup>-</sup>TCR<sup>high</sup> thymocytes, gated as in Supporting Information Fig. S2B. Depicted gates were used to quantify recirculating Treg. (D) Quantification of recirculating Treg. Each symbol represents the mean of 7–14 individual measurements  $\pm$  SD, pooled from one to four independent experiments per time-point. See Supporting Information Fig. S2C for absolute numbers. ns, not significant; \* $p < 0.05$ ; \*\* $p < 0.01$ ; \*\*\* $p < 0.001$ ; \*\*\*\* $p < 0.0001$  (Mann–Whitney test). (E) Confocal microscopy of medullary sections of thymi of *Rag2-Gfp Foxp3-Thy1a*

of recirculating Tconv among CD4SP thymocytes were somewhat higher in NOD than in B6 thymi up to 6 weeks of age and substantially higher at 7 and 8 weeks (Supporting Information Fig. S2E–G). However, we previously showed that fully mature recirculating Tconv do not quantitatively alter Treg development [15], and therefore did not further investigate this issue.

Using confocal microscopy, we found recirculating Treg almost exclusively in the thymic medulla (Supporting Information Fig. S2H), suggesting that the proportion of recirculating Treg among CD4SP cells should reflect the density of these cells within the thymic medulla. To verify this issue, we analyzed by confocal microscopy the density of recirculating Treg in the thymic medullae of NOD and B6 mice. Cortical and medullary areas were distinguished based on expression levels of GFP, high in cortical CD4<sup>+</sup>CD8<sup>+</sup> double positive and lower in medullary CD4 or CD8 single positive thymocytes. In agreement with the flow cytometry data (Fig. 2C and D), we observed approximately twofold higher densities of recirculating GFP<sup>+</sup> Treg in the medullae of NOD than in those of B6 thymi, at 3 and 8 weeks of age (Fig. 2E and F).

Combined, these data show that NOD mice have a larger thymic Treg-niche than B6 mice (Fig. 1A) and that substantially more recirculating Treg accumulate in the thymus of NOD than of B6 mice (Fig. 2D; Supporting Information Fig. S2H). The size of this niche in NOD and B6 thymi is quite stable from 2 to 8 weeks of age (Supporting Information Fig. S2I). By contrast, its composition is much more dynamic. In agreement with the literature [15], an increase in recirculating cells and a drop in developing cells are observed with age, more so in NOD than in B6 mice (Supporting Information Fig. S2I).

### Thymic recirculating Treg in NOD and B6 mice have similar phenotypes

To identify the reason(s) for the greater levels of recirculating Treg in the NOD as compared to the B6 thymus, we first analyzed and compared their phenotypes at 3 weeks of age. In agreement with previous findings [14,15], we found that whereas newly developing GFP<sup>+</sup> Treg had mostly a naive phenotype (Supporting Information Fig. S3A), many recirculating GFP<sup>+</sup> Treg displayed a CD44<sup>high</sup>CD62L<sup>low</sup> activated/memory phenotype (Fig. 3A). Sizeable proportions of recirculating (but not newly developing) Treg in NOD and B6 thymi also expressed the surface markers CD103, TIGIT, and ST2, all associated with Treg activation (Fig. 3A; Supporting Information S3A). Most GFP<sup>+</sup> Treg also expressed CXCR4, a chemokine receptor implicated in Treg re-entry into the thymus, whereas GFP<sup>+</sup> Treg expressed lower levels (Fig. 3B). Despite their medullary localization, recirculating GFP<sup>+</sup> Treg expressed lower levels of CCR7 than newly developing GFP<sup>+</sup> Treg. Interestingly,

whereas most GFP<sup>+</sup> Treg in B6 mice expressed CCR6, as previously reported [25], a sizeable proportion of recirculating Treg in NOD mice did not. The latter observation emphasizes the need for identification of more reliable markers for newly developing versus recirculating Treg in WT mice.

mRNA-sequencing analysis of GFP<sup>+</sup> Treg from NOD and B6 thymi revealed only 491 genes that were differentially expressed in NOD versus B6 recirculating Treg (Fig. 3C). We found some differences in the expression of genes differentially expressed between resting and activated Treg [26] (Fig. 3D). However, examination of the thus identified genes did not reveal any obvious reason for the difference in recirculation (Supporting Information Fig. S3B and Table S1). We did not find a statistically significant difference in expression of this gene-set as a whole neither (Fig. 3D). Examination of selected gene-sets involved in T cell-development, -activation, or -differentiation, in lymphocyte-homing, or in Treg-effector functions only revealed one with a statistically significant difference ( $p < 0.05$ , FDR  $< 0.25$ ) between NOD and B6 recirculating Treg: “regulation of IL-17 production” (Supporting Information Table S2), which is not obviously linked to Treg-recirculation. Unsupervised gene-ontology analysis of the 491 differentially expressed genes did not reveal any obvious link to Treg-recirculation neither (Supporting Information Fig. S3C and Table S3).

Taken together, these phenotype and transcriptome data indicate a great similarity between the recirculating Treg found in the thymi of NOD versus B6 mice. They thus did not reveal information on why we found more recirculating Treg in the NOD than in the B6 thymus.

### Increased activation of Treg in the periphery of NOD mice promotes their greater recirculation to the thymus

It was previously shown that mainly activated T cells migrate back to the thymus [27]. The activated phenotype of recirculating GFP<sup>+</sup> Treg in B6 [14,15] and NOD (Fig. 3) mice is consistent with this observation. The higher levels of recirculating Treg in the NOD as compared to the B6 thymus may therefore be due to greater activation of Treg in the periphery of NOD mice. To test this hypothesis, we compared the phenotype of fully mature (GFP<sup>+</sup>) splenic NOD and B6 Treg by flow cytometry. We found substantially higher proportions of CD44<sup>high</sup>CD62L<sup>low</sup> activated/memory cells among splenic Treg in NOD than in B6 mice (Fig. 4A; Supporting Information Fig. S4A). We also examined the proportion of differentiated, CD103<sup>+</sup> cells within the mature splenic Treg population. Again, we found substantially more CD103<sup>+</sup> cells among GFP<sup>+</sup> Treg in NOD than in B6 mice (Fig. 4B). Expression of ST2, a component of the receptor for IL-33, identifies a population

NOD and B6 mice. Cortex and medulla were distinguished based on GFP intensity level (green). The white arrow denotes a developing Treg, the yellow one a recirculating Treg. Three independent samples were analyzed per condition. Recirculating GFP<sup>+</sup>Foxp3<sup>+</sup> Treg were quantified using Imaris-software. The scale bar in the lower left panel represents 5  $\mu$ m. (F) Density of recirculating Treg in the medulla of NOD and B6 thymi. Each symbol represents one individual mouse per experiment with three to five different sections analysed. \* $p < 0.05$ ; \*\*\* $p < 0.001$  (Student t-test).

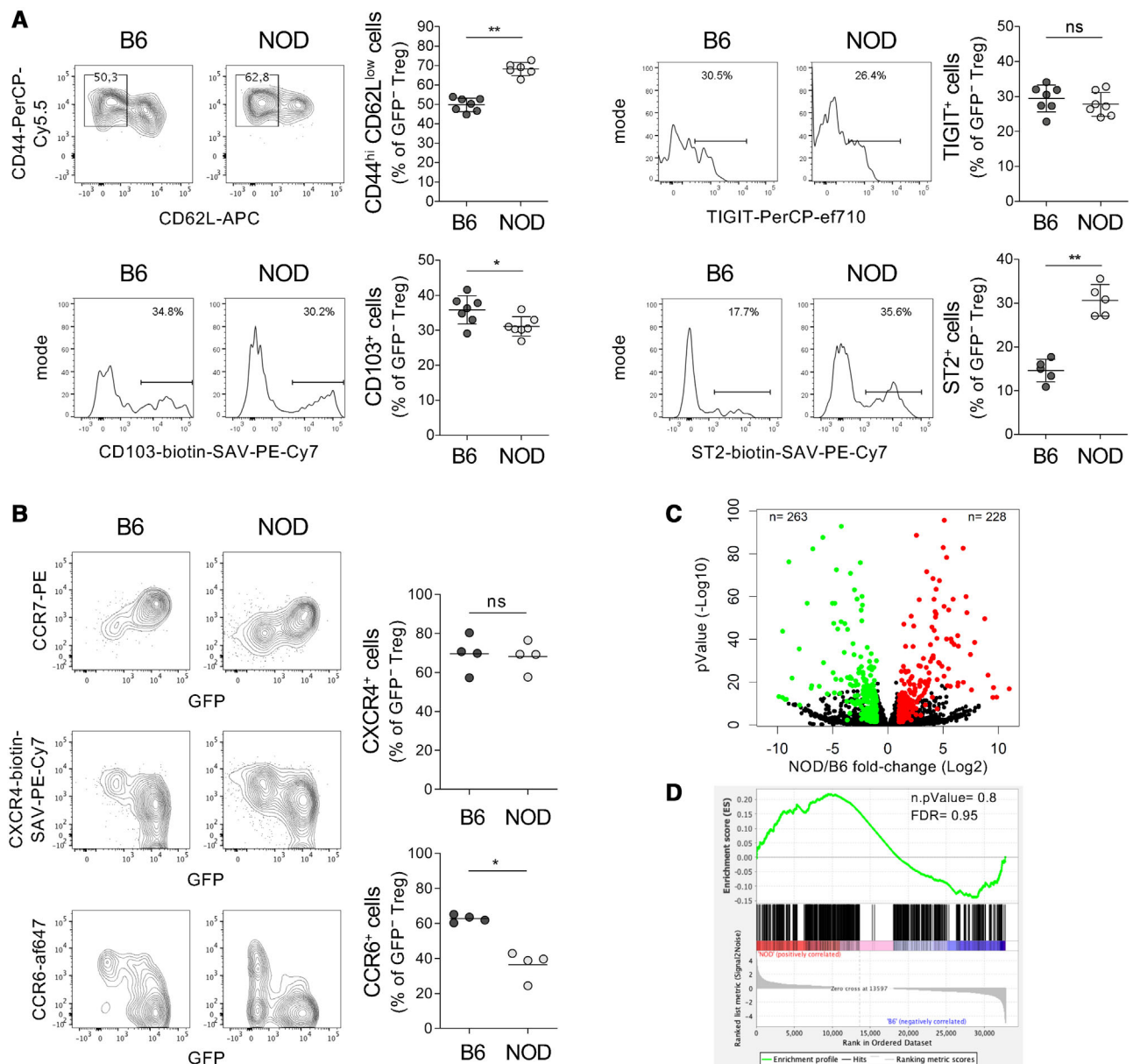


**Figure 3.** Similarity between recirculating thymic Treg in B6 and NOD mice. (A and B) Flow-cytometry analyses of electronically gated CD4<sup>+</sup> CD8<sup>-</sup> GFP<sup>-</sup> Thy1.1<sup>+</sup> recirculating thymic Treg from *Rag2-Gfp Foxp3-Thy1a* NOD and B6 mice. Antibodies against indicated surface molecules were used in addition to the ones used for identification of the recirculating Treg. Each symbol indicates a single animal. Data are from one experiment on mice 3-weeks-of-age, similar results were obtained in an independent experiment with mice 2-weeks-of-age. ns, not significant; \* $p < 0.05$ ; \*\* $p < 0.01$  (Mann–Whitney test). (C and D) Transcriptomic analysis (RNAseq) of FACS-sorted CD4<sup>+</sup> CD8<sup>-</sup> TCR<sup>high</sup> GFP<sup>-</sup> Thy1.1<sup>+</sup> recirculating thymic Treg from *Rag2-Gfp Foxp3-Thy1a* NOD and B6 mice. (C) Volcano plot showing the differentially expressed genes. FC, NOD/B6 fold change; n, number of differentially expressed genes (adjusted  $p < 0.05$ , normalized counts  $> 100$ , green  $FC \leq 0.5$ , red  $FC \geq 2$ ). (D) Enrichment plot for the “Treg activation signature” gene-set [26] is shown. The enrichment score and the gene-ranking correspond to NOD versus B6. FDR, false discovery rate. Three independent biological replicates (each containing cells from 8 to 17 pooled NOD and B6 thymi) were analyzed.

of highly suppressive Treg preferentially localized in tissues [3]. We found much higher proportions of ST2<sup>+</sup> cells among GFP<sup>-</sup> splenic Treg in NOD than in B6 mice (Fig. 4C). Taken together, these data show that the fraction of Treg displaying a highly activated and differentiated phenotype is substantially higher in the periphery of NOD than that of B6 mice. A higher level of recirculating Treg in the NOD than in the B6 thymus therefore correlates

with a higher proportion of activated cells among Treg in the periphery.

To assess if the correlation between the levels of activated Treg in the periphery and recirculating cells in the thymus is a general phenomenon, we analyzed the proportions of activated cells among peripheral CD4<sup>+</sup> Foxp3<sup>+</sup> Treg in eight inbred mouse-strains and compared it to the proportions of recirculating

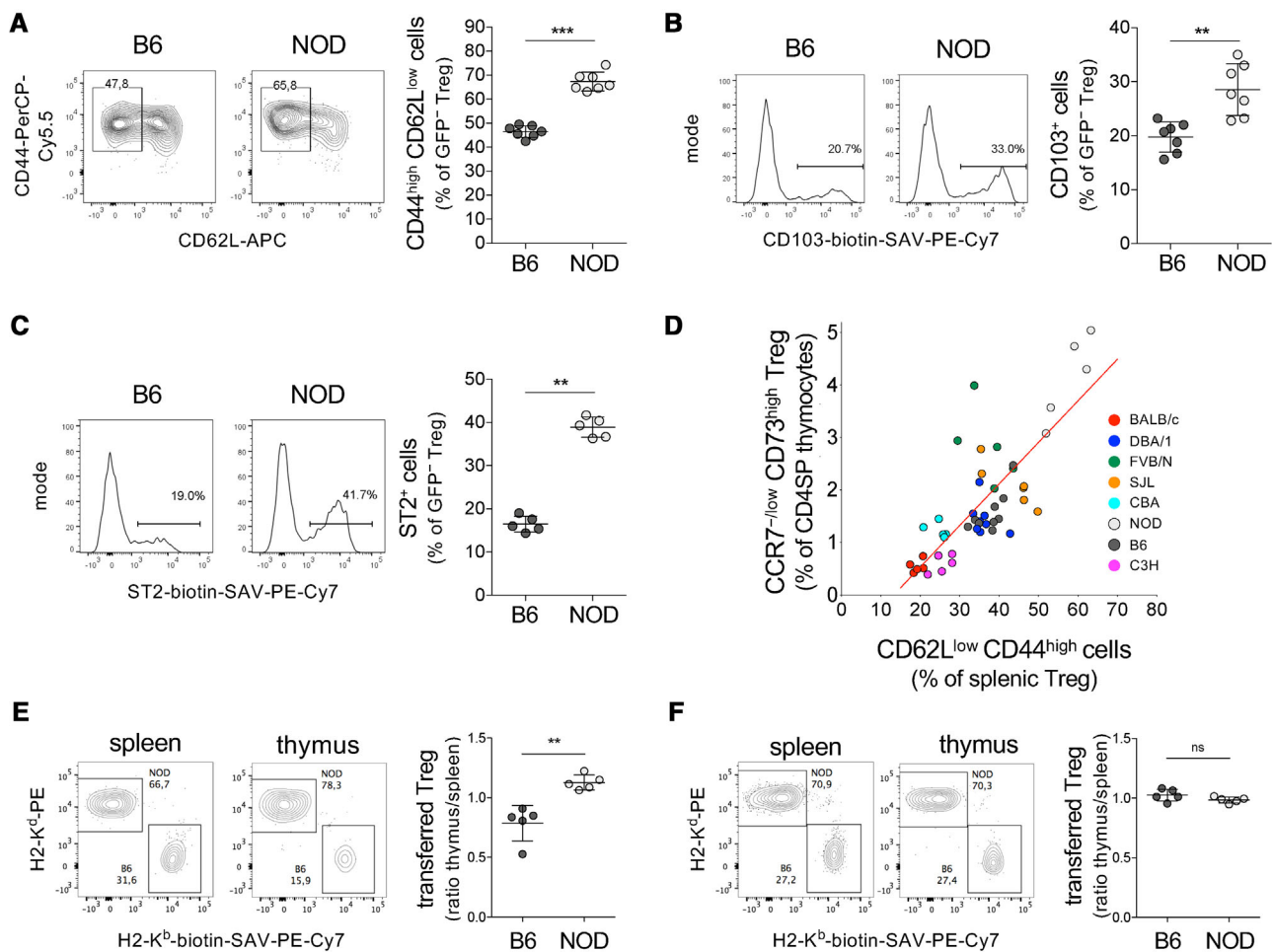


**Figure 4.** Hyperactivation of peripheral NOD Treg explains their greater recirculation back to the thymus. (A–C) Flow-cytometry analyses of electronically gated  $CD4^+ CD8^- GFP^- Thy1.1^+$  splenic Treg using antibodies to these and indicated markers. Depicted electronic gates were used for the quantifications shown in the right panels. Each symbol indicates a single animal. Data are from two independent experiments. (D) Thymocytes from WT animals of the indicated inbred mouse strains were analyzed by flow-cytometry using antibodies to indicated markers. Shown are the proportions of activated  $CD62L^{low} CD44^{high}$  cells among  $CD4^+ CD8^- Foxp3^+$  Treg in the spleen versus recirculating  $CCR7^{-/low} CD73^{high} Foxp3^+$  Treg among  $CD4^+ CD8^- TCR^{high}$  (CD4SP) cells in the thymus. The red line indicates a linear regression curve,  $R^2 = 0.63$ ,  $p < 0.0001$ . Five to nine mice were analyzed for each strain in two to three independent experiments. (E) Treg freshly isolated from spleens of *Rag2-Gfp Foxp3-Thy1a* NOD and B6 mice were co-injected i.v. into  $(B6 \times NOD)F_1$  hosts. Twenty-four hours later, injected  $Thy1.1^+$  NOD ( $H-2K^d$ ) and B6 ( $H-2K^b$ ) Treg were identified in indicated organs by flow-cytometry using antibodies to indicated markers. Numbers near gates indicate the frequency (%) among injected cells. A representative experiment is shown. Right panel: Efficiency of migration of injected NOD and B6 Treg to the thymus is expressed as ratio of these cells found in the thymus versus spleen. Each symbol indicates a single animal, results are from three independent experiments. (F) As in (E), but Treg were activated ex vivo prior to injection. Mean values  $\pm$  SD. ns, not significant; \* $p < 0.05$ ; \*\* $p < 0.01$ ; \*\*\* $p < 0.001$  (Mann-Whitney test).

$CCR7^{-/low} CD73^{high}$  Treg among CD4SP thymocytes in these mice. We thus found a direct correlation between the levels of activated Treg in the spleen and recirculating Treg in the thymus (Fig. 4D).

This observation suggests that the higher proportions of recirculating ( $GFP^-$ ) cells we found among Treg in the NOD as compared to the B6 thymus was due to the substantially higher frequencies of activated cells among peripheral Treg in NOD mice. To directly test this hypothesis, we adoptively transferred Treg and assessed their migration to the thymus. We purified Treg from peripheral lymphoid organs of 3-week-old *Foxp3-Thy1a* mutant NOD and B6 mice and injected a mix of them i.v. into NK-cell-depleted  $(NOD \times B6) F_1$  hosts. The day after, we analyzed the accumulation of transferred Treg in the spleen and the thymus

(Fig. 4E). The proportion of NOD and B6 cells among transferred Treg found in the spleen was taken as the proportion of surviving injected cells. NOD and B6 Treg-migration to the thymus was expressed as the ratio of the percentages of NOD or B6 cells among transferred Treg found in the thymus versus spleen. As shown in Fig. 4E, proportionally more NOD than B6 Treg had migrated to the thymus. These data may be explained by our observation that there are more activated cells among NOD than among B6 Treg. To directly assess this possibility, we ex vivo pre-activated NOD and B6 Treg, adoptively transferred them into  $(NOD \times B6) F_1$  hosts, and analyzed their migration to thymus. The results demonstrate that ex vivo activated NOD and B6 Treg equally efficiently migrated to the thymus (Fig. 4F).



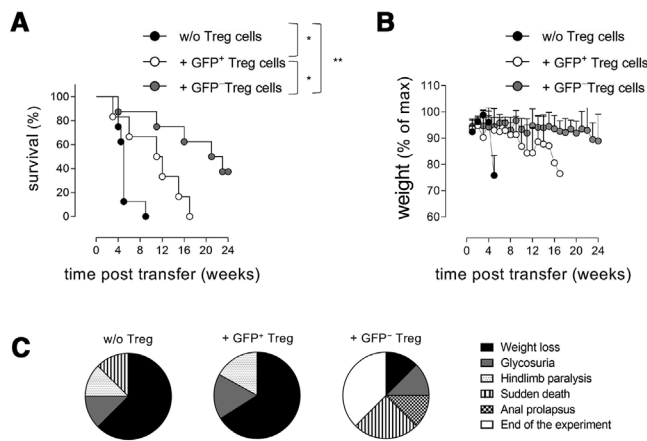


**Figure 5.** Recirculating intrathymic Treg protect better from immunopathology than freshly developing Treg. Treg-depleted splenocytes were injected in NOD  $C\alpha^0$  mice alone (w/o Treg cells) or complemented, to original Treg-proportions, with GFP<sup>+</sup> or GFP<sup>-</sup> thymic Treg. (A) Survival (see Materials and Methods section) and (B) weight of the mice was monitored over time (mean values  $\pm$  SD). w/o Treg cells,  $n = 8$  individuals; +GFP<sup>+</sup> Treg cells,  $n = 6$  mice; +GFP<sup>-</sup> Treg cells,  $n = 8$  mice, data are pooled from two (w/o Treg) to three (+Treg) independent experiments. Log Rank (Mantel-Cox) test: ns, not significant; \* $p < 0.05$ ; \*\* $p < 0.001$ . (C) Camembert-chart indicating the cause of death of experimental animals.

Taken together, these data indicate that the greater proportions of recirculating Treg we found in the NOD than in the B6 thymus were not due to an intrinsic difference in the ability of activated Tregs from NOD mice to home to and accumulate in the thymus, but rather a reflection of the higher proportion of activated Tregs in the periphery of NOD mice.

### Recirculating NOD Treg protect better against experimental immunopathology than newly developing cells

Since (presumably antigen-driven) peripheral activation strongly favors Treg recirculation back to the thymus, we hypothesized that recirculating Treg have a more pronounced *in vivo* function than newly developing cells. To assess this postulate, we performed adoptive transfer experiments. *Foxp3-Thy1a* mutant splenocytes were depleted of Thy1.1<sup>+</sup> Treg and subsequently reconstituted (or not) with thymic GFP<sup>+</sup> or GFP<sup>-</sup> Treg to original levels of Treg. These cells were i.v. injected into  $C\alpha$ -mutant NOD mice, which lack TCR $\alpha\beta$ -expressing T cells. The control group receiving only Treg-depleted splenocytes rapidly died. Co-injection of GFP<sup>+</sup> Treg delayed mortality. Interestingly, co-injection of GFP<sup>-</sup> Treg delayed mortality substantially more (Fig. 5A). In contrast to the mice that had received thymic GFP<sup>+</sup> Treg, which lost weight over time, the weight of the mice that had received GFP<sup>-</sup> Treg remained stable during the whole duration of the experiment (24 weeks, Fig. 5B). Determination of the symptoms of pathology developing in the mice of the three experimental groups confirmed that thymic GFP<sup>-</sup> Treg controlled pathology better than their GFP<sup>+</sup> counterparts (Fig. 5C). Taken together, these data show that recir-

culating thymic Treg are particularly capable of protecting against immunopathology.

### Greater accumulation of recirculating Treg in NOD thymus leads to stronger inhibition of Treg development

As shown in Fig. 2B, higher levels of Treg developed in the thymi of 2- and 3-week-old NOD than B6 thymi. However, starting at 4 weeks of age, the levels of Treg development in these two mouse-strains were indistinguishable. Treg development appears therefore more inhibited with age in NOD than in B6 mice. We previously showed that recirculating Treg inhibit the de novo development of Treg in FTOC and in B6 mice [15]. Analysis of the levels of CCR7<sup>-/low</sup> CD73<sup>high</sup> recirculating and CCR7<sup>high</sup> CD73<sup>-/low</sup> newly developing Treg in the eight inbred mouse strains revealed an inverse correlation between these two parameters (Fig. 6A), supporting our conclusion that recirculating Treg inhibit the de novo development of Treg.

We previously reported that recirculating Treg inhibit development of Foxp3<sup>+</sup> Treg but not of Foxp3<sup>-</sup> CD25<sup>+</sup> precursors [15]. In agreement with this conclusion, we found that, whereas the proportions of Foxp3<sup>-</sup> CD25<sup>+</sup> thymocytes dropped both in B6 and NOD mice, the decline was similar in B6 and NOD mice (Supporting Information Fig. S5).

The stronger decline in Treg development in NOD than in B6 mice (Fig. 2B) is therefore likely caused by the higher proportions of recirculating Treg we found in the NOD than in the B6 thymus (Fig. 2D). However, it may also be due to a hypothetical higher intrinsic capacity of recirculating NOD Treg to inhibit de novo Treg development. To assess the latter possibility, we analyzed the correlation between the levels of recirculating and newly developing Treg in the thymi of B6 and NOD mice. To compare Treg-development in thymi with similar levels of recirculating Treg in the thymus, we used data from B6 mice of 2–53 weeks of age and from NOD mice of 2–8 weeks of age. The correlation of recirculating versus newly developing NOD Treg essentially paralleled that of B6 cells (Figs. 6B and C). This result suggests that the intrinsic capacity of recirculating NOD Treg to inhibit de novo development of Treg is not different from that of B6 cells, which is consistent with their quite similar phenotypes (Fig. 3).

If the decline in Treg development we observed in NOD thymi is caused by recirculating Treg, decreasing the levels of the latter cells should increase Treg development. To assess this, we repeatedly i.v. injected anti-CD4 antibody for 3 weeks to deplete peripheral CD4<sup>+</sup> T cells. This treatment substantially reduced the proportions of conventional and of regulatory CD4<sup>+</sup> T cells in the spleen (Supporting Information Fig. S6A). Whereas thymic cellularities were unaltered (Supporting Information Fig. S6B), we observed a substantial reduction in the levels of recirculating GFP<sup>-</sup> Treg in the thymus (Figs. 6D and E). Whereas the proportions of the distinct populations of developing thymocytes, including CD4SP cells, did not change in anti-CD4 treated mice (Supporting Information Fig. S6C), we observed a significant increase in the

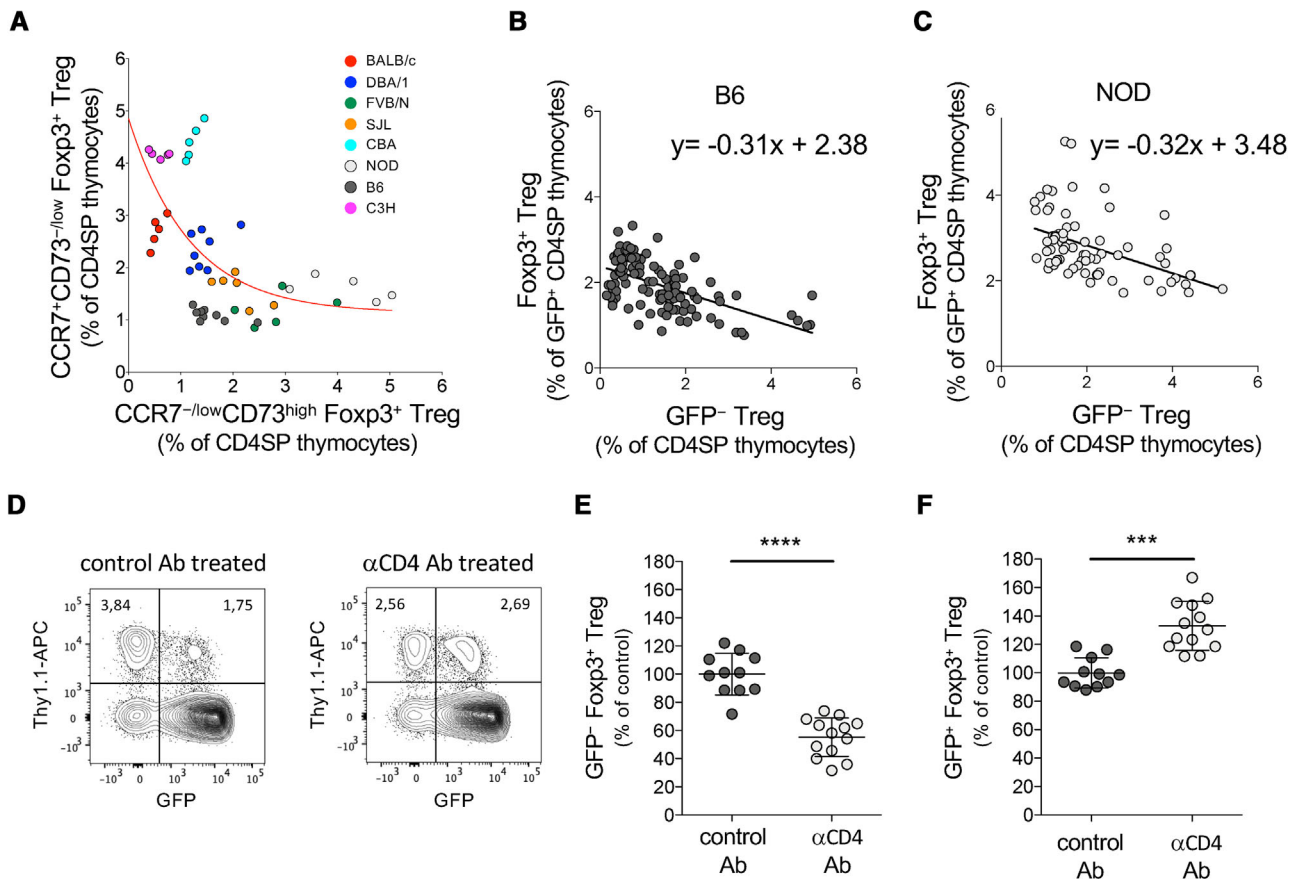


**Figure 6.** Recirculating Treg in the thymus inhibit de novo development of Treg. (A) Thymocytes from 8-week-old mice of the indicated inbred mouse-strains were analyzed by flow-cytometry using antibodies to indicated markers. The proportions of recirculating  $CCR7^{-/low} CD73^{high}$  versus newly developing  $CCR7^{high} CD73^{-/low} Fopx3^{+}$  Treg among  $CD4^{+} CD8^{-} TCR^{high}$  (CD4SP) thymocytes are depicted for each individual mouse analyzed. The red line indicates a one-phase regression curve,  $R^2 = 0.37$ . Five to nine mice were analyzed for each strain in two to three independent experiments (B and C) Thymocytes from *Rag2-Gfp Fopx3-Thy1a* B6 and NOD mice were analyzed by flow-cytometry. The proportions of recirculating  $GFP^{-}$  versus newly developing  $GFP^{+} Thy1.1^{+}$  Treg among  $CD4^{+} CD8^{-} TCR^{high}$  (CD4SP) thymocytes are depicted for each individual mouse analyzed. To compare mice with similar proportions of recirculating Treg in the thymus, B6 mice were of 2–53 weeks of age, NOD mice of 2–8 weeks of age. Each symbol indicates a single animal. Data are pooled from 29 (B) and 21 (C) independent experiments. Linear regression curves and their equations are shown. (D) Three-week-old *Rag2-Gfp Fopx3-Thy1a* NOD mice were injected with anti-CD4 (or control) antibody every 3 days during 3 weeks. Their thymocytes were analyzed by flow cytometry at day 21 after the first injection. GFP versus Thy1.1 expression by electronically gated CD4SP thymocytes. (E) Indicated are the proportions of recirculating  $GFP^{-}$  Treg among CD4SP thymocytes (upper-left quadrant in D) as percentages of the mean values found in the mice of the control group, for each performed experiment ( $n = 11$  control and 13 treated mice from three independent experiments). (F) As in (E), but indicated are the proportions of newly developing  $GFP^{+}$  Treg. Bars indicate mean values  $\pm$  SD.  $***p < 0.001$ ;  $****p < 0.0001$  (Mann-Whitney test).

proportions of developing Treg (Fig. 6D and F). These data thus consolidate our conclusion that, as we previously showed for B6 mice [15], in NOD mice recirculating Treg inhibit intrathymic de novo Treg-development.

## Discussion

Here, we show that in the type I diabetes-prone NOD mouse-strain the thymic niche for Treg is, paradoxically, exceptionally large. Consistently, the capacity of thymic precursors to develop into Treg is greater in NOD mice than in most other inbred mouse-strains we studied. However, relatively large proportions of Treg are activated in the NOD periphery and these cells migrate back to

the thymus. This leads to a relatively strong inhibition of de novo Treg development in the NOD thymus. As a consequence, Treg development in adult NOD mice is quantitatively quite similar to that in adults of several other inbred mouse strains. Thus, very dynamic mechanisms quantitatively control Treg development in the thymus and link this process to activation of Treg in peripheral tissues and organs.

Our results are in apparent opposition with reports documenting enhanced thymic development of Treg in NOD mice through life [19,22]. However, previous work did not take into account the heterogeneity of the thymic Treg population, composed of developing cells and, with age, ever larger proportions of peripheral Treg that had recirculated back to the thymus [15]. In the current study, the use of *Rag2-Gfp* mice allowed us to perform a

longitudinal analysis and comparison of the amount of de novo generated thymic Treg in NOD and B6 mice. While enhanced Treg development was observed in NOD thymi during the first 3 weeks of life, consistent with previous reports [19,22], comparable proportions of developing Treg were seen in the two strains from 4 weeks-of-age on. These results emphasize the importance of distinguishing differentiating and recirculating cells when studying Treg development in the thymus.

If and how these findings affect the peripheral repertoire and function of NOD Treg remains to be determined. Recent work underlined the key role of neonatal Treg in protection of the organism from fatal immune diseases [28]. Since recirculating Treg inhibit the development of new Treg from 3 to 4 weeks of age on, this mechanism should not affect the generation of neonatal Treg. However, it may be linked to the observation that Treg developing later on inefficiently protect from lethal autoimmune pathology in the experimental system used by these authors. A strong decline in Treg production early in life may contribute to the generation of a more restricted repertoire of TCR expressed by NOD than B6 Treg, as suggested by the work of Ferreira [29], which could impair peripheral Treg responses.

Several groups reported that mostly activated T cells migrate back to the thymus (reviewed in [27]). Our results indicate that heightened activation of peripheral NOD Treg explains their increased recirculation back to the thymus early in life. We indeed observed exceptionally high amounts of effector and differentiated Treg in the periphery of young NOD as compared to seven other inbred mouse strains, directly correlating with the levels of recirculating cells in the thymus. Moreover, in adoptive transfer experiments of ex vivo activated NOD and B6 Treg, these cells displayed comparable capabilities to recirculate back to the thymus. At least two hypotheses can explain the hyper-activation of peripheral neonatal NOD Treg. (I) It has been previously suggested that NOD mice are lymphopenic [30]. Since the repertoire of Treg (but not Tconv) is enriched in self-reactive cells [31], these cells could expand more in NOD than B6 mice. However, adoptive transfer experiments in lymphopenic hosts have actually shown that NOD Treg proliferate less than their B6 counterparts [32]. (II) Alternatively, the repertoire of NOD Treg may be more auto-reactive than the one of B6 mice, resulting in a greater activation of NOD than B6 peripheral Treg. This hypothesis is supported by a study showing an enrichment in self-reactive CD4<sup>+</sup> T cells in NOD (as compared to B6) mice [33]. It is tempting to speculate that thymic selection of high affinity/avidity Treg leads to their peripheral activation and expansion [34] and, as a consequence, to their recirculation back to the thymus where they suppress de novo development of Treg.

It was previously shown that autospecific Treg are activated in the periphery [34]. Given that mainly activated T cells re-enter the thymus [27], the recirculating Treg therefore presumably are, at least in part, autospecific. In support of this hypothesis, we found that recirculating Treg protect better against immunopathology than newly developing cells, which have not undergone this “selection-process” in the periphery. This observation suggests that recirculating Treg in the thymus reflect (auto-)immune-responses

going on in the periphery. They may therefore contribute to a hypothetical modulation of T cell-selection by peripheral immune responses, as previously hypothesized for cytotoxic T cells [35]. This hypothesis would merit further investigation.

Interestingly, in seven and 8-week-old thymi from NOD but not B6 mice, we also observed substantially greater proportions of Tconv that had recirculated from the periphery back to the thymus. This observation probably correlates with increasing peripheral activation of NOD T cells with age, insulinitis starting in 3-week-old animals and progressing over time [36]. It was recently shown that recirculating Tconv, via RANK signaling, boost mTEC differentiation ultimately leading to exhaustion of TEC precursors [37]. Increased recirculation of regulatory and conventional T cells, both expressing high levels of RANKL [15,37], could therefore contribute to the accelerated thymic involution and medulla disorganization observed in NOD mice [38].

In conclusion, enhanced peripheral activation of Treg in young NOD mice results in their increased migration back to the thymus where they inhibit the development of new Treg. It will be important in the future to determine if and how recirculating Treg, for example, by interacting with thymic stromal cells, modify the specificity-based selection of developing thymocytes. This process could contribute to the reported age-related change in the development of autoreactive T cells observed in NOD mice [39].

## Materials and methods

### Mice

*Rag2-Gfp* B6 mice [13] were kindly provided by Pamela Fink and *Foxp3-Thy1a* B6 mice [40] by Adrian Liston. *Rag2-Gfp* B6 mice and *Foxp3-Thy1a* B6 mice were speed-backcrossed to NOD/LtJ as previously reported [41]. After reaching NOD homozygosity for all the *Idd*-loci tested (5–6 generations), additional backcross to NOD/LtJ was performed for 10 generations. Glycosuria was routinely tested. Animals were considered diabetic when their glycosuria was  $\geq 0.5$  g/dL. Positive mice were excluded from the analysis. NOD/LtJ and CD45.1 B6 mice were used to generate (NOD $\times$ B6) F1 animals. NOD/C $\alpha^{\circ}$  (NOD.129P2(C)-*Tcra*<sup>tm1Mjo</sup>/DoiJ) mice were kindly provided by Dr. Sylvie Guerder and originally obtained from JAX laboratories. BALB/cJ, CBA, C3H/HE, DBA/1, and FVB/N mice were obtained from Janvier; SJL mice were from Charles River. All experiments involving animals were performed in compliance with governmental and institutional guidelines (ethical approval APAFIS#4151-201602171 0481496.v6).

### Antibodies

The following monoclonal antibodies (mAbs) and secondary reagents were used: Pacific Blue-labeled anti-CD4 (GK1.5), Biotin-labeled anti-CD4 (RM4.4), PE-CF594-labeled anti-CD8 $\alpha$

(53.6.7), PE-Cy7- and PE-labeled anti-CD25 (PC61), Biotin-labeled anti-TCR $\beta$  (H57-597), APC-labeled anti-Thy1.1 (OX-7), AF647-labeled CCR6 (140706) (all from BD Bioscience); Biotin-labeled anti-Thy1.1 (HIS51), PE-labeled anti-TCR $\beta$  (H57-597), PE-Cy7-labeled or PerCpCy5.5-labeled or APC-EF780-labeled anti-CD44 (IM7), APC or PE-labeled anti-CD62L (MEL-14), PE-Cy7- or PE-labeled streptavidin, Biotin-labeled anti-CD103 (2E7), PerCp-ef710-labeled anti-TIGIT (GIGD7), PE-labeled anti-H-2K<sup>d</sup> (SF1-1.1), Biotin-labeled anti-H-2K<sup>b</sup> (AF6-88.5), Biotin-labeled anti-ST2 (RMST2-2), Biotin-labeled anti-CXCR4 (2B11), PE-labeled anti-CCR7 (4B12), EF660-labeled anti-Foxp3 (FJK16S) (all from eBioscience); and BV605-labeled anti-CD73 (TY/11.8) (from Biolegend).

### Flow cytometry

Sample preparation and staining were essentially performed as previously described [42]. FACS data were acquired using an LSRII or a Fortessa flow cytometer (BD Biosciences, San Jose, CA) and analyzed using FlowJo software (Tree Star, Ashland, OR). Doublets and dead cells were excluded from the analysis by using appropriate FSC/SSC gates. For CCR7 and CXCR4 staining, cells were incubated in complete medium with CCR7- or CXCR4-specific antibodies during 45 min at 37°C, and 45 min at RT for CCR6.

### Purification of Treg

Splenocytes and LN cells from 3-week-old NOD and B6 *Rag2-Gfp Foxp3-Thy1a* mice were depleted of erythrocytes and incubated with a mixture of anti-Fc $\gamma$ RIII/Fc $\gamma$ RII (2.4G2), anti-CD8 $\alpha$  (H59), anti-MHC-II (M5/114), and anti-B220 (RA3-6B2) antibodies (all purified from hybridoma culture supernatants). Labeled cells were eliminated with anti-rat IgG antibody-coated Dynabeads (Invitrogen). The resulting population was stained with APC-labeled anti-Thy1.1 and then incubated with anti-APC microbeads (Miltenyi Biotec) and positively selected using MS columns (Miltenyi Biotec). Purity (>95%) and activation status were assessed by flow cytometry. Thus purified Treg cells were transferred into recipient mice, either directly after purification or after ex vivo activation.

### Ex vivo activation of Treg cells

Purified B6 and NOD *Rag2-Gfp Foxp3-Thy1a*<sup>+</sup> Treg cells were cultured in 96-well round-bottom plates coated with anti-CD3 $\epsilon$  (2C11, 5  $\mu$ g/mL) and anti-CD28 (37.51, 1  $\mu$ g/mL) (BioXcell) mAbs in the presence of IL-2 (500 U/mL) (Roche). After 2 days, cells were transferred to uncoated 96-well flat-bottom plates and cultured for five additional days in the presence of IL-2 (500 U/mL). At day 7, Treg cells were harvested and adoptively transferred.

### Treg cell adoptive transfer

Freshly purified or ex vivo activated B6 and NOD Treg cells were mixed at a 1:1 ratio. (NODxB6) F1 recipient mice were injected i.p. with 100  $\mu$ g of anti-NK-1.1 mAb (PK136, BioXcell) to deplete NK cells and, 24 h later, i.v. injected with Treg cells ( $4 \times 10^6$  cells/mouse). Twenty-four hours after adoptive transfer, the spleen and thymus of the recipient mice were collected and thymocytes were depleted of CD8<sup>+</sup> cells using an anti-CD8 $\alpha$  hybridoma (31M) supernatant and rabbit complement. Cells were then labeled with indicated antibodies and analyzed by flow cytometry. Injected cells were identified as CD4<sup>+</sup>Thy1.1<sup>+</sup>; NOD and B6 cells were identified as expressing H-2K<sup>d</sup> and H-2K<sup>b</sup>, respectively.

### Confocal microscopy

Thymi from 3- and 8-week-old *Rag2-Gfp Foxp3-Thy1a* B6 and NOD mice were fixed overnight in a 2% paraformaldehyde solution at 4°C. Thymi were then washed in PBS and dehydrated in successive sucrose baths (10, 20, and 30% in PBS). Organs were then embedded in TissueTek OCT compound (Sakura, Japan) and frozen. Blocks were mounted into a cryostat (Leica, Germany) and 6  $\mu$ m-thick sections were collected. Sections were rehydrated in PBS, permeabilized with 0.1% Triton X-100 in PBS and stained with directly labeled antibodies overnight at 4°C, followed, if applicable, by streptavidin staining for 4 h at 4°C. Sections were mounted in Mowiol mounting medium (Sigma-Aldrich) and images acquired with a Leica SP8 confocal microscope with a 63 $\times$  objective. Images were analyzed with Imaris scientific software (Bitplane, USA). The GFP intensity of cortical and medullary thymocytes was calculated for a spot 4  $\mu$ m in diameter for every Foxp3<sup>+</sup> CD4<sup>+</sup> cell. For determination of background values of GFP intensity, spots 4  $\mu$ m in diameter were analyzed in interstitial regions of the thymus. Cortical and medullary regions were distinguished based on the GFP intensity of the thymocytes (cortex  $\geq 80$  > medulla).

The following antibodies were used: Pacific Blue-labeled anti-CD4 (RM4-5) (BD Bioscience); EF660-labeled anti-Foxp3 (FJK-16S), EF570-labeled anti-Foxp3 (FJK-16S) (both from eBioscience), and AF488 labeled anti-GFP (A-21311) (Invitrogen).

### RNA sequencing and data analysis

After complement or magnetic bead-mediated depletion of CD8<sup>+</sup> cells, GFP<sup>-</sup> CD4<sup>+</sup> Thy1.1<sup>+</sup> Treg were FACS-sorted from thymi of 3-week-old *Rag2-Gfp Foxp3-Thy1a* male B6 and NOD mice. Total RNA was extracted with miRNeasy micro kit (Qiagen, USA) and its quality was controlled using an Agilent 2100 BioAnalyzer (Agilent technologies, USA). Three independent biological replicates (each containing cells from 8 to 17 pooled NOD and B6 thymi) were analyzed. Libraries for RNA-sequencing (RNA-seq) were prepared using the TruSeq Standard Total RNA LT protocol

(Illumina, USA), using 50–100 ng of high-quality RNA (RIN > 8.5). The quality of each library was checked using an Agilent 2100 BioAnalyzer. Samples were indexed and sequenced on Illumina HiSeq3000.

The reads were trimmed with the Trimmomatic tool [43], after which they were aligned to the mouse reference genome mm10 (GRCm38.95) plus the alternative patch of this genome (GRCm38.dna.alt.fa), and quantified, using STAR (v.2.6) [44]. Differential expression analysis and normalization of the counts were performed using DESeq2 (v.1.16.1) [45]. Genes with an adjusted *p*-value < 0.05 (Benjamini & Hochberg), fold change > 2, and mean normalized counts > 100 in at least one strain were selected (depicted in Fig. 3D). For Fig. 3C and Supporting Information Table S3, the Gene set enrichment analysis was performed with the normalized counts of the three replicates of NOD and B6 mice, the enrichment score is NOD/B6. The gene sets were selected from the GO terms knowledgebase (biological process), or from published data: “Treg canonical signature” and “Treg activation signature” [26], “Recirculating Treg signature” [15], “Treg perinatal signature” [28], and “Th1-Th2-Th17 signature” [46]. In Supporting Information Fig. S3B, the heatmaps were generated normalizing the mean to zero and a variance of  $\log_2(1.2)$  per gene and graphed with the package “heatmap.2.” An unsupervised Gene ontology analysis was performed using the web tool GOrilla [47], and the enriched terms (shown in Supporting Information Table S2) were then treated with the web tool REVIGO [48] to group the redundant terms. The RNAseq data are available in the Gene Expression Omnibus (GEO) database (<http://www.ncbi.nlm.nih.gov/gds>) under the accession number GSE145713, the R scripts are available in [https://github.com/arielgalindoalbarran/NOD\\_Treg\\_recirculation](https://github.com/arielgalindoalbarran/NOD_Treg_recirculation).

### Adoptive transfer into NOD $C\alpha^0$ mice

Splenocytes of 10–13-week-old prediabetic *Rag2-Gfp Foxp3-Thy1a* NOD mice were depleted of erythrocytes and then incubated with APC-labeled anti-Thy1.1 mAb (OX7) and anti-APC microbeads (Miltenyi Biotec). Treg cells were then depleted using a sensitive depletion program (depl025) on the Automacs Pro Separator (Miltenyi Biotec). Eleven- to 16-week-old NOD  $C\alpha^0$  mice were injected with  $10^6$  Treg-depleted splenocytes alone (control group) or reconstituted (to original proportions) with GFP<sup>+</sup> (developing) or GFP<sup>-</sup> (recirculating) Treg (CD4<sup>+</sup> Thy1.1<sup>+</sup>) cells, FACS-sorted from thymi of 2–3-week-old *Rag2-Gfp Foxp3-Thy1a* NOD mice. Weekly, glycosuria and weight loss were monitored. Mice tested positive for glycosuria, that lost 20% of their maximal body weight, or that showed signs of suffering (e.g., hunched body), were euthanized. Remaining mice were euthanized 24 weeks after adoptive transfer, and necropsy was performed. Mice that had developed macroscopically visible lymphomas (i.e., thymoma, severe spleno-, or lymphadenomegaly), a pathology previously described in lymphopenic NOD mice [49,50], were excluded from the analysis.

### In vivo CD4 T-cell-depletion

Three-week-old NOD mice were injected i.p. with anti-CD4 (GK1.5, BioXCell) or isotype matched control (ratIgG2b/ $\kappa$ , BioXCell) antibodies. Mice were first injected with 0.2 mg of antibody and then received 0.1 mg of antibody every 3 days during the next 3 weeks. Their splenocytes and thymocytes were analyzed by flow cytometry at day 21 after the first injection.

**Acknowledgments:** The authors thank Pamela Fink for *Rag2-Gfp* mice, Adrian Liston for *Foxp3-Thy1a* mice, and Sylvie Guerder for NOD  $C\alpha^0$  mice and for constructive discussions. The authors are also very grateful to the following persons for excellent technical assistance: Fatima L’Faqihi, Valérie Duplan-Eche, Anne-Laure Iscache, Lidia De la Fuente, and Paul Menut of the CPTP Cytometry platform; Olivier Bouchez of the GeT-PlaGE Genotoul; and the personnel of the Inserm US006 ANEXPLO/Creffre animal facility. The authors are grateful to all the members of the ‘T-cell mediated immune Tolerance team’ for discussion and input in the project. J.P.M.v.M. is grateful to the staff of the Biochemistry Institute of the Lausanne University, Epalinges, Switzerland, for its hospitality. This work was financially supported by the Fondation pour la Recherche Médicale (to J.v.M., DEQ20160334920; to J.C.S., FDT201904008280); the IdEx Toulouse (to E.R. and P.R.); the Région Midi Pyrénées (to J.v.M., 15/06/12.05); and the Agence Nationale pour la Recherche (to P.R., ANR-16-CE15-0015-01). J.D., J.C.S., A.G.A., E.A.R., O.P.J., and J.P.M.v.M. dedicate this work to the memory of their late, much respected and regretted colleague, P.R.

**Conflict of interest:** The authors declare no commercial or financial conflict of interest.

### References

- 1 Sakaguchi, S., Miyara, M., Costantino, C. M. and Hafler, D. A., FOXP3+ regulatory T cells in the human immune system. *Nat. Rev. Immunol.* 2010. 10: 490–500.
- 2 Josefowicz, S. Z., Lu, L. - F. F. and Rudensky, A. Y., Regulatory T cells: mechanisms of differentiation and function. *Annu. Rev. Immunol.* 2012. 30: 531–564.
- 3 Panduro, M., Benoist, C. and Mathis, D., Tissue Tregs. *Annu. Rev. Immunol.* 2016. 34: 609–633.
- 4 Bennett, C. L., Christie, J., Ramsdell, F., Brunkow, M. E., Ferguson, P. J., Whitesell, L., Kelly, T. E. et al., The immune dysregulation, polyendocrinopathy, enteropathy, X-linked syndrome (IPEX) is caused by mutations of FOXP3. *Nat. Genet.* 2001. 27: 20–21.
- 5 Brunkow, M. E., Jeffery, E. W., Hjerrild, K. A., Paeper, B., Clark, L. B., Yasayko, S. A., Wilkinson, J. E. et al., Disruption of a new

- forkhead/winged-helix protein, scurfy, results in the fatal lymphoproliferative disorder of the scurfy mouse. *Nat Genet.* 2001. 27: 68–73.
- 6 Klein, L., Robey, E. A. and Hsieh, C. - S., Central CD4(+) T cell tolerance: deletion versus regulatory T cell differentiation. *Nat. Rev. Immunol.* 2019. 19: 7–18.
- 7 Romagnoli, P. and van Meerwijk, J. P. M., Thymic selection and lineage commitment of CD4(+)Foxp3(+) regulatory T lymphocytes. *Prog. Mol. Biol. Transl. Sci.* 2010. 92: 251–277.
- 8 Tai, X., Cowan, M., Feigenbaum, L. and Singer, A., CD28 costimulation of developing thymocytes induces Foxp3 expression and regulatory T cell differentiation independently of interleukin 2. *Nat. Immunol.* 2005. 6: 152–162.
- 9 Mahmud, S. A., Manlove, L. S., Schmitz, H. M., Xing, Y., Wang, Y., Owen, D. L., Schenkel, J. M. et al., Costimulation via the tumor-necrosis factor receptor superfamily couples TCR signal strength to the thymic differentiation of regulatory T cells. *Nat. Immunol.* 2014. 15: 473–481.
- 10 Coquet, J. M., Ribot, J. C., Bąbala, N., Middendorp, S., van der Horst, G., Xiao, Y., Neves, J. F. et al., Epithelial and dendritic cells in the thymic medulla promote CD4+Foxp3+ regulatory T cell development via the CD27-CD70 pathway. *J. Exp. Med.* 2013. 210: 715–28.
- 11 Marski, M., Kandula, S., Turner, J. R. and Abraham, C., CD18 Is Required for Optimal Development and Function of CD4 + CD25 + T Regulatory Cells. *J. Immunol.* 2005. 175: 7889–7897.
- 12 Apert, C., Romagnoli, P. and van Meerwijk, J. P. M. J. P. M., IL-2 and IL-15 dependent thymic development of Foxp3-expressing regulatory T lymphocytes. *Protein Cell.* 2018. 9: 322–332.
- 13 Yu, W., Nagaoka, H., Jankovic, M., Misulovin, Z., Suh, H., Rolink, A., Melchers, F. et al., Continued RAG expression in late stages of B cell development and no apparent re-induction after immunization. *Nature* 1999. 400: 682–7.
- 14 McCaughy, T. M., Wilken, M. S. and Hogquist, K. A., Thymic emigration revisited. *J. Exp. Med.* 2007. 204: 2513–2520.
- 15 Thiault, N., Darrigues, J., Adoue, V., Gros, M., Binet, B., Perals, C., Leobon, B. et al., Peripheral regulatory T lymphocytes recirculating to the thymus suppress the development of their precursors. *Nat. Immunol.* 2015. 16: 628–634.
- 16 Yang, E., Zou, T., Lechner, T. M., Zhang, S. L. and Kambayashi, T., Both retention and recirculation contribute to long-lived regulatory T-cell accumulation in the thymus. *Eur. J. Immunol.* 2014. 44: 2712–2720.
- 17 Weist, B. M., Kurd, N., Boussier, J., Chan, S. W. and Robey, E. A., Thymic regulatory T cell niche size is dictated by limiting IL-2 from antigen-bearing dendritic cells and feedback competition. *Nat. Immunol.* 2015. 16: 635–41.
- 18 Nikolouli, E., Elfaki, Y., Herppich, S., Schelmbauer, C., Delacher, M., Falk, C., Mufazalov, I. A. et al., Recirculating IL-1R2+ Tregs fine-tune intrathymic Treg development under inflammatory conditions. *Cell. Mol. Immunol.* 2020: 1–12.
- 19 Feuerer, M., Jiang, W., Holler, P. D., Satpathy, A., Campbell, C., Bogue, M., Mathis, D. et al., Enhanced thymic selection of FoxP3+ regulatory T cells in the NOD mouse model of autoimmune diabetes. *Proc. Natl. Acad. Sci. U. S. A.* 2007. 104: 18181–18186.
- 20 Romagnoli, P., Tellier, J. and van Meerwijk, J. P. M., Genetic control of thymic development of CD4+CD25+FoxP3+ regulatory T lymphocytes. *Eur. J. Immunol.* 2005. 35: 3525–3532.
- 21 Tellier, J., van Meerwijk, J. P. and Romagnoli, P., An MHC-linked locus modulates thymic differentiation of CD4+CD25+Foxp3+ regulatory T lymphocytes. *Int. Immunol.* 2006. 18: 1509–1519.
- 22 Tellier, J., Andrianjaka, A., Vicente, R., Thiault, N., Enault, G., Garchon, H. J., van Meerwijk, J. P. M. et al., Increased thymic development of regulatory T cells in NOD mice is functionally dissociated from type I diabetes susceptibility. *Eur. J. Immunol.* 2013. 43: 1356–1362.
- 23 Wyss, L., Stadinski, B. D., King, C. G., Schallenberg, S., McCarthy, N. I., Lee, J. Y., Kretschmer, K. et al., Affinity for self antigen selects Treg cells with distinct functional properties. *Nat. Immunol.* 2016. 17: 1093–1101.
- 24 Smigiel, K. S., Richards, E., Srivastava, S., Thomas, K. R., Dudda, J. C., Klonowski, K. D. and Campbell, D. J., CCR7 provides localized access to IL-2 and defines homeostatically distinct regulatory T cell subsets. *J. Exp. Med.* 2014. 211: 121–136.
- 25 Cowan, J. E., McCarthy, N. I. and Anderson, G., CCR7 controls thymus recirculation, but not production and emigration, of Foxp3+ T cells. *Cell Rep.* 2016. 14: 1041–1048.
- 26 Joller, N., Lozano, E., Burkett, P. R., Patel, B., Xiao, S., Zhu, C., Xia, J. et al., Treg cells expressing the coinhibitory molecule TIGIT selectively inhibit proinflammatory Th1 and Th17 cell responses. *Immunity* 2014. 40: 569–81.
- 27 Hale, J. S. and Fink, P. J. Back to the thymus: peripheral T cells come home. *Immunol. Cell. Biol.* 2009. 87: 58–64.
- 28 Yang, S., Fujikado, N., Kolodin, D., Benoist, C. and Mathis, D., Regulatory T cells generated early in life play a distinct role in maintaining self-tolerance. *Science* 2015. 348: 589–594.
- 29 Ferreira, C., Singh, Y., Furmanski, A. L., Wong, F. S., Garden, O. A. and Dyson, J., Non-obese diabetic mice select a low-diversity repertoire of natural regulatory T cells. *Proc. Natl. Acad. Sci. U. S. A.* 2009. 106: 8320–8325.
- 30 King, C., Ilic, A., Koelsch, K. and Sarvetnick, N., Homeostatic expansion of T cells during immune insufficiency generates autoimmunity. *Cell* 2004. 117: 265–277.
- 31 Romagnoli, P., Hudrisier, D. and van Meerwijk, J. P. M., Preferential recognition of self antigens despite normal thymic deletion of CD4+CD25+ regulatory T cells. *J. Immunol.* 2002. 168: 1644–1648.
- 32 Le Campion, A., Gagnerault, M., Auffray, C., Bécourt, C., Lallemand, E., Bienvendu, B., Martin, B. et al., Lymphopenia-induced spontaneous T-cell proliferation as a cofactor for autoimmune disease development. *Blood* 2013. 114: 1784–1793.
- 33 Stadinski, B. D., Shekhar, K., Gómez-Touriño, I., Jung, J., Sasaki, K., Sewell, A. K., Peakman, M. et al., Hydrophobic CDR3 residues promote the development of self-reactive T cells. *Nat. Immunol.* 2016. 17: 946–55.
- 34 Fisson, S., Darrasse-Jeze, G., Litvinova, E., Septier, F., Klatzmann, D. and Liblau, R., Salomon, B. L., Continuous activation of autoreactive CD4+CD25+ regulatory T Cells in the steady state. *J. Exp. Med.* 2003. 198: 737–746.
- 35 Edelman, S. L., Marconi, P. and Brocker, T., Peripheral T cells re-enter the thymus and interfere with central tolerance induction. *J. Immunol.* 2011. 186: 5612–5619.
- 36 Andre, I., Gonzalez, A., Wang, B., Katz, J., Benoist, C. and Mathis, D., Checkpoints in the progression of autoimmune disease: lessons from diabetes models. *Proc. Natl. Acad. Sci. U. S. A.* 1996. 93: 2260–2263.
- 37 Yin, C., Pei, X. - Y., Shen, H., Gao, Y. - N., Sun, X. - Y., Wang, W., Ge, Q. et al., Thymic homing of activated CD4+ T cells induces degeneration of the thymic epithelium through excessive RANK signaling. *Sci. Rep.* 2017. 7: 2421.
- 38 Atlan-Gepner, C., Naspetti, M., Valéro, R., Barad, M., Lepault, F., Vialettes, B. and Naquet, P., Disorganization of thymic medulla precedes evolution towards diabetes in female NOD mice. *Autoimmunity* 1999. 31: 249–260.
- 39 He, Q., Morillon, 2nd Y. M., Spidale, N. A., Kroger, C. J., Liu, B., Sartor, R. B., Wang, B. et al., Thymic development of autoreactive T cells in NOD mice is regulated in an age-dependent manner. *J. Immunol.* 2013. 191: 5858–5866.

- 40 Liston, A., Nutsch, K. M., Farr, A. G., Lund, J. M., Rasmussen, J. P. and Koni, P. A., Rudensky, A. Y., Differentiation of regulatory Foxp3<sup>+</sup> T cells in the thymic cortex. *Proc. Natl. Acad. Sci. U. S. A.* 2008. **105**: 11903–11908.
- 41 Viret, C., Leung-Theung-Long, S., Serre, L., Lamare, C., Vignali, D. A., Malissen, B., Carrier, A. et al., Thymus-specific serine protease controls autoreactive CD4 T cell development and autoimmune diabetes in mice. *J. Clin. Invest.* 2011. **121**: 1810–1821.
- 42 Cossarizza, A., Chang, H. - D., Radbruch, A., Acs, A., Adam, D., Adam-Klages, S., Agace, W. W. et al., Guidelines for the use of flow cytometry and cell sorting in immunological studies (second edition). *Eur. J. Immunol.* 2019. **49**: 1457–1973.
- 43 Bolger, A. M., Lohse, M. and Usadel, B., Trimmomatic: A flexible trimmer for Illumina sequence data. *Bioinformatics* 2014. **30**: 2114–2120.
- 44 Dobin, A., Davis, C. A., Schlesinger, F., Drenkow, J., Zaleski, C., Jha, S., Batut, P. et al., STAR: Ultrafast universal RNA-seq aligner. *Bioinformatics* 2013. **29**: 15–21.
- 45 Anders, S., Huber, W., Differential expression analysis for sequence count data. *Genome Biol.* 2010. **11** R106.
- 46 Araujo Furlan, C. L., Boari, J. T., Rodriguez, C., Canale, F. P., Vernengo, F. F., Boccardo, S., Beccaria, C. G. et al., Limited Foxp3<sup>+</sup> regulatory T cells response during acute *Trypanosoma cruzi* infection is required to allow the emergence of robust parasite-specific CD8<sup>+</sup> T cell immunity. *Front. Immunol.* 2018. **9**: 2555.
- 47 Eden, E., Navon, R., Steinfeld, I., Lipson, D. and Yakhini, Z., GOrilla: A tool for discovery and visualization of enriched GO terms in ranked gene lists. *BMC Bioinformatics* 2009. **10**: 48.
- 48 Supek, F., Bošnjak, M., Škunca, N. and Šmuc, T., Revigo summarizes and visualizes long lists of gene ontology terms. *PLoS One* 2011. **6**: e21800.
- 49 Chiu P. P. L., Ivakine E., Mortin-Toth S. and Danska J. S., Susceptibility to lymphoid neoplasia in immunodeficient strains of nonobese diabetic mice. *Cancer Res.* 2002. **62**: 5828–5834.
- 50 Prochazka M., Gaskins H. R., Shultz L. D. and Leiter E. H., The nonobese diabetic scid mouse: model for spontaneous thymomagenesis associated with immunodeficiency. *Proc. Natl. Acad. Sci. U. S. A.* 1992. **89**: 3290–3294.

**Abbreviations:** B6: C57BL/6 · CD4SP: CD4<sup>+</sup>CD8<sup>-</sup>TCR<sup>high</sup> thymocyte · NOD: non-obese diabetic · Tconv: conventional T lymphocyte · Treg: regulatory T lymphocyte

**Full correspondence:** Joost P.M. van Meerwijk, Inserm U1043, BP 3028, 31024 Toulouse Cedex 3, France.  
e-mail: Joost.van-Meerwijk@inserm.fr

The peer review history for this article is available at <https://publons.com/publon/10.1002/eji.202048743>

Received: 20/5/2020

Revised: 3/7/2020

Accepted: 28/7/2020

Accepted article online: 30/7/2020